Electronic Noise in Semiconductor-Based Radiation Detection Systems: A Comprehensive Analysis With a Unified Approach

Giuseppe Bertuccio, *Member, IEEE*, and Filippo Mele, *Member, IEEE*

***Abstract*— The electronic noise is a key-issue during the phases of design, integration, and characterization of a detection system for ionizing radiation, as it determines both its ultimate and actual performances. The precise identification and quantification of all noise sources and associated components allow to implement specific strategies for their control and minimization during the system design and manufacturing phases, to disentangle all noise contributions, and to verify their correspondence with the expectations during the system characterization. An effective approach to the electronic noise problem requires to consider in detail all the parts of the detection system but it is not so rare to still observe that the electronic noise is erroneously confused or interpreted as the noise of the electronics or as the quadratic sum of the electronics' and detector's noise, usually reducing the latter to that one associated with its dark current only. In this article, a detailed analysis of the noise model of a radiation detection system employing a semiconductor detector is presented using a unified approach which takes into account all sources and causes of electronic noise and their reciprocal interaction. The noise related to the generation, transport, and loss of the signal charge in the detector is analyzed in detail and, in particular, the charge trapping and detrapping processes, showing how their contributions could be not negligible even in detectors based on high purity semiconductors. The unified approach allows to disclose the interplay between the detector, the interconnection, and the front-end electronics (FEEs) showing that some noise contributions cannot be attributed exclusively to a single part, but it is correct to refer to them as system noises. Several examples taken from experimental data are presented and discussed and a method to determine the dielectric noise introduced by the interconnection and the detector is described. The concept of equivalent noise energy (ENE) is formalized revealing how it is useful to compare systems employing detectors made with different semiconductors and eventually affected by charge trapping. The analysis is developed assuming semiconductor detectors but can be easily applied to system using other types of radiation detectors.**

***Index Terms*— Charge sensitive preamplifiers, electronic noise, front end electronics, low-noise amplifiers, nuclear electronics, radiation detectors, semiconductor device noise, semiconductor radiation detectors.**

Manuscript received 3 August 2023; accepted 23 August 2023. Date of publication 31 August 2023; date of current version 24 October 2023. This work was supported in part by the European Union through the project "FSE REACT-EU, PON Ricerca e Innovazione 2014–2020."

The authors are with the Department of Electronics, Information and Bioengineering, Politecnico di Milano, 22100 Como, Italy, and also with the Italian National Institute of Nuclear Physics (INFN), 20133 Milan, Italy (e-mail: giuseppe.bertuccio@polimi.it; filippo.mele@polimi.it).

Color versions of one or more figures in this article are available at https://doi.org/10.1109/TNS.2023.3310357.

Digital Object Identifier 10.1109/TNS.2023.3310357

I. Introduction

THE problem of the electronic noise in systems devoted to the detection, spectroscopy, or imaging of ionizing radiation has been the subject of continuous studies and research activities since the birth of nuclear electronics and it is treated in all related classical books and publications [1], [2], [3], [4], [5], [6], [7], [8], [9], [10], [11], [12], [13]. The focus of the study has been always aimed at the development of systems with the lowest electronic noise in order to detect low-energy particles or to achieve the highest energy, timing, or position resolution in spectroscopy, detection, or imaging of radiation. Historically, the problem was initially directed at the development of low-noise thermionic tube preamplifiers for the almost noiseless ionization chambers [14], [15] and continued when the semiconductor detectors were conceived and developed [16], [17], [18], almost simultaneously with the transition between vacuum tube and solid-state electronics [19], [20], [21], [22]. Maybe for this historical context, even today the idea that the front-end electronics (FEEs) is responsible for most of the electronic noise of the radiation detection systems is still widespread, so that *electronic noise* and *noise of electronics* are considered almost synonyms. The fact that the electronic noise is directly associated with amplifiers has a historical explanation. It might be useful to point out that the noise is said "electronic" not because it is associated with the readout electronics of the system, but because it regards the spontaneous fluctuations in the phenomenon of generation and/or transport or thermal agitation of electric charges into any electrical device. These fluctuations were observed and explained for the first time in 1918 by W. Schottky in the plate current of vacuum tubes and were called "shot effect" [23]. The wording "electronic noise" was originally coined later, at the beginning of XX century, in analogy and as cause of the familiar "acoustic noise" heard in the telephone receivers when the first vacuum-tube amplifiers were employed, generating the then called "tube noise" [24], so that a certain direct association between *electronic noise* and *amplifiers* was set since the beginning, although also the microphones (equivalent to "acoustic wave detectors") used in telephones were source of electronic noise, as well. Since then, many different electronic devices have been invented and different noise sources associated with electrical and electronic components

© 2023 The Authors. This work is licensed under a Creative Commons Attribution-NonCommercial-NoDerivatives 4.0 License.
For more information, see https://creativecommons.org/licenses/by-nc-nd/4.0/

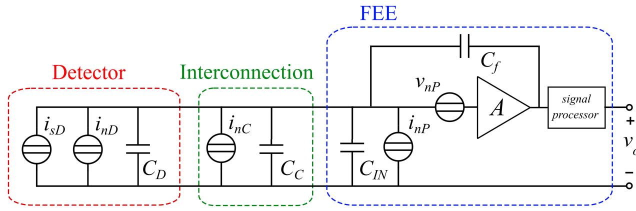

Fig. 1. Model of an energy-to-voltage radiation detection system for evaluating the electronic noise. The radiation induced current at the readout electrode is modeled by the i_{sD} generator, v_{nP}, i_{nD}, i_{nC}, and $_{inP}$ are the input referred series voltage and parallel current noise components of the detection system. C_D, C_C, C_{IN}, and C_f are the capacitances of the detector, connection, preamplifier input, and feedback, respectively. A is a voltage amplifier.

have been identified and studied. In the case of radiation detection systems, the common approach to the electronic noise issue considers the noise mainly originated by the readout electronics, while the detector and interconnection are believed to cover a secondary rule. This approach has brought to the consequence that the electronic noise issue is mainly addressed by experts in FEEs, while the problem is interesting for all the scientists and engineers involved in detector and system designs, manufacturing, testing, and applications. Another approach would be to evaluate the system noise as the combination of two main independent components, the first arising from the detector, the latter from the FEEs. This article aims to overcome the above limitations by presenting an analysis of the electronic noise problem with a unified approach, with a particular attention to the detector and interconnection, revealing the interplay between the different parts of the system. Although semiconductor detectors are considered in the following, the analysis can be easily extended also to other type of detectors.

II. Noise Model of a Detection System

A. Introduction

In Fig. 1, the general noise model for a radiation detection system constituted by a semiconductor detector connected to the FEE is shown. The detector is represented with an ideal current source generating the signals i_{sD} and the capacitance C_D of its output electrode. The readout FEE includes the charge preamplifier and the filter (shaper) stages. The preamplifier is modeled with its input C_{IN} and feedback C_f capacitances. The interconnection between the detector output and the FEE input, generally realized with a simple conducting wire or a bump bonding, is modeled with its capacitance C_C toward ground, valid in all cases in which the series resistance and inductance of the interconnection are negligible.

The electronic noise sources present in the system can be modeled with four generators: two of them (v_{nP}, i_{nP}) account for all noise sources present within the FEE, i_{nD} and i_{nC} represent the noise sources within the detector and related to the interconnection, respectively. With respect to i_{sD}—the signal source—v_{nP} is in series and so it is called "series (voltage) noise" while (i_{nP}, i_{nD}, i_{nC}) are in parallel with i_{sD}, and so are indicated as "parallel (current) noise."

It is worthwhile to point out that the *electronic noise generators* in Fig. 1 model any spontaneous and random fluctuation of the voltage or current in the network, independently of the origin of these fluctuations. Specifically, v_{nP}, i_{nP} model the effect of all fluctuations originating within the electrical elements (transistors, resistors, ...) of the FEE and affecting the output voltage v_o. i_{nD} models the fluctuations originating inside the detector by different phenomena and affecting the detector output current. Furthermore, i_{nD} is not only associated with the dark current, but also to all the fluctuations arising from the generation and the transport processes of the charge generated by the radiation. The i_{nD} generator can include also the noise associated with a multiplication process of the transported charge, as in low gain avalanche diodes (LGADs) [25]. The generator i_{nC} models the current fluctuations associated with the interconnection. In the following, each of these electronic noise components is discussed, examining its peculiarity and its effect on the system performance.

B. Equivalent Noise Charge

Let us first recall the concept of equivalent noise charge (*ENC*), useful in the following discussion. The FEE output signal is generally a voltage pulse whose peak amplitude $v_o = kQ_{\mathrm{ind}}$ is proportional to the total electric charge Q_{ind} induced at the output electrode of the detector hit by a photon/particle, with k [F^{-1}] being the charge-to-voltage conversion factor. First assuming, for an ideal signal source, that a photon/particle with a given energy generates always a charge Q_s not affected by any fluctuation, the signal to noise ratio (S/N) at the system output is determined by the output noise measured with its r.m.s. value $v^{\mathrm{out}}_{n(\mathrm{rms})}$, that is

$$\frac{S}{N} = \frac{v_o}{v^{\mathrm{out}}_{n(\mathrm{rms})}} = \frac{kQ_s}{v^{\mathrm{out}}_{n(\mathrm{rms})}}. \tag{1}$$

It is useful to describe the system noise not in terms of $v^{\mathrm{out}}_{n(\mathrm{rms})}$ but with its equivalent quantity of charge injected at the system input, so-called *equivalent noise charge* $ENC = v^{\mathrm{out}}_{n(\mathrm{rms})}/k$. Therefore, the *ENC* defines the quantity of signal charge at the detector-output/FEE-input for which the SNR at the FEE output is unity [13]. The *ENC* is a useful quantity because, for a given value of signal Q_s, the S/N at the system output can be simply evaluated as $S/N = Q_s/ENC$ as given by (29).

C. ENC Equation

The *ENC* of the detection system modeled in Fig. 1 is evaluated with the well-known equation [13], [26]

$$ENC_{\mathrm{EN}} = \sqrt{A_1 S_V C_T^2 \frac{1}{\tau} + A_2\left(2\pi A_f C_T^2 + \frac{B_f}{2\pi}\right) + A_3 S_I \tau} \tag{2}$$

in which τ is usually the shaping or the peaking time of the shaper and A_1, A_2, and A_3 are numerical coefficients dependent on the type of pulse shaping,[1] whose values for three most common shaping are reported in Table I. S_V and S_I are the power spectral densities of the series voltage and parallel current white noises, respectively; A_f is a factor related to the series voltage $1/f$ noise; B_f accounts for the noise associated with dielectric losses of all capacitances; C_T is the total capacitance at the common node detector output/FEE

[1] A_i coefficients values can be found in [13] for mathematical noise power spectral densities (npsd). In case physical npsd are assumed, as in the following, the A_i values are halved with respect to those reported in [13].

TABLE I

A_1, A_2, AND A_3 NOISE SHAPING COEFFICIENTS

Shaping Function	A1	A2	A3
Triangular	1	0.44	0.33
Trapezoidal ($\tau_{peak} = \tau_{flat-top}$)	1	0.69	0.84
Semi-Gaussian (3rd order)	1.02	0.53	0.9

Noise shaping coefficients as computed on monolateral (physical) power spectral densities.

input of the system, given by the sum of the detector output capacitance C_D, the interconnection capacitance C_C, and the FEE total capacitance $C_P = C_{\mathrm{IN}} + C_f$

$$C_T = C_D + C_C + C_P. \tag{3}$$

It is worthwhile to observe that the *ENC*, as expressed by (2), takes into account only the fluctuations generated by v_{nP}, i_{nP}, and i_{nD} limited to the detector dark current noise, and i_{nC} as due to dielectric noise. Since these are considered as the classical sources of electronic noise, the subscript EN has been used for *ENC* in (2). ENC_{EN} does not account for any fluctuation arising from the processes of generation and transport of the signal electric charges, which will be considered in Section V.

Experimentally, ENC_{EN} can be evaluated by measuring the full width at half maximum (FWHM) of the line generated by a precision pulser injecting known electric charge packets at the FEE input. Equation (2) is written in a particular form which highlights the τ-dependence of the different noise components and it can be used to determine the noise parameters and the total capacitance of a detection system (S_V, S_I, A_f, B_f, C_T) by fitting the experimental ENC_{EN} versus τ data [27].

III. Detector, Electronics, and System Noise

In this section, (2) will be rewritten in other forms, which allows to better highlight other peculiarities, which are interesting for the analysis of the system noises. Specifically, (2) can be rewritten by putting in evidence two contributions, the first one due to the series voltage noise and the latter due to the parallel current noise components

$$ENC_{\mathrm{EN}} = \sqrt{ENC_S^2 + ENC_P^2} \tag{4}$$

in which the series and parallel components are derived by (2) as follows:

$$ENC_S^2 = A_1 S_V C_T^2 \frac{1}{\tau} + A_2 2\pi A_f C_T^2 \tag{5}$$

$$ENC_P^2 = A_2 \frac{B_f}{2\pi} + A_3 S_I \tau. \tag{6}$$

In Sections III-A–III-E, the parallel ENC_P and series ENC_s components will be analyzed and discussed in detail emphasizing some interesting aspects.

A. Parallel Noise: The Dielectric Component

The parallel noise component ENC_P given by (6) is determined by the sum of two parts: the first one due to the dielectric current noise [26], the latter due to the current white noise. The dielectric noise component, whose effect on charge amplifiers was originally studied by V. Radeka in the '70's [28], [29], arises from all insulating materials adjacent or in direct contact to the detector-output/FEE-input node; these mainly include the printed circuit board (PCB), the dielectrics of the preamplifier's feedback capacitance and input transistor. The *ENC* due to a capacitor C_{die} with a lossy dielectric is given by [26]

$$ENC_D = \sqrt{A_2 2kT D C_{\mathrm{die}}} \tag{7}$$

in which D is the dissipation factor which ranges from 10^{-5} to 10^{-2} depending on the material, giving ENC_D values from a few electrons to several tens of electrons [11], [26]. Separating the three dissipation factors for the three capacitances constituting C_T (3), and equating the dielectric component in (2) with (7), the coefficient B_f can be explicitly written as follows:

$$B_f = \pi 4kT(D_D C_D + D_C C_C + D_P C_P) \tag{8}$$

and (6) can be written as follows:

$$ENC_P^2 = A_2 2kT(D_D C_D + D_C C_C + D_P C_P) + A_3 S_I \tau \tag{9}$$

which highlights that also the parallel noise component has a dependence on all the capacitive components of the system.

B. Parallel Noise: The White Component

In the second component of (6), arising from the current white noise, the spectral density S_I can be divided in two parts: S_{ID} given by the detector and S_{IP} given by the FEE, which can be written as follows:

$$S_{ID} = 2qI_D \tag{10}$$

$$S_{IP} = 2qI_P + \frac{4kT}{R_P} + a(2qI_{DS}) \tag{11}$$

in which q is the elementary electric charge and I_D is the dark current at the detector output electrode. Equation (10) assumes that the dark current shows a pure shot noise, so that no excess noise for charge multiplication occurs in the detector as well as no noise suppression due to space charge effects [30]. I_P is the leakage current at preamplifier input, which can be significant in case of preamplifiers using a bipolar junction transistor (BJT) as input transistor [31] or low but non-negligible in case of deep sub-micrometer MOSFETs, MESFETs or HEMTs [26], [32]. R_P is the equivalent noisy resistance connected at the preamplifier input, associated with the feedback resistance and/or the resistance used to bias the detector output electrode, if present. The third term includes the so-called non-stationary current noise because it depends on the signal amplitude and rate [33]. For continuous reset preamplifiers with diodes or subthreshold MOSFETs, the coefficient is $a = 1$ and $I_{DS} = I_D + \overline{I_S} + I_B$ is the sum of the detector dark current (I_D), the mean value of the signal current ($\overline{I_S}$) flowing through the reset device and eventually a DC bias current (I_B) of the reset device [34]. It is worthwhile to note that this component is a combination of detector and FEE interplay because, if the noise source is located within the reset device, the noise is induced and determined by the detector through

I_{DS}. In case the charge preamplifier employs a pulsed reset $a = 0$; however, pulsed reset preamplifiers can suffer from an additional noise contribution known as kTC noise, arising from the sampling of the thermal noise of the switch resistance on the feedback capacitance at the end of the reset phase [35], and can suffer also from stability issues that might result in similar fluctuations on the output baseline level [36]. These noise contributions can, however, be removed by filtering the low-frequency band of the noise spectrum, which can be done using an AC coupling or time-variant filtering techniques such as correlated double sampling (CDS) [35].

C. Total Parallel Noise

In conclusion, the parallel noise component ENC_P given by (6) can be rewritten as follows:

$$ENC_P^2 = A_2\frac{B_f}{2\pi} + A_3 S_{ID}\tau + A_3 S_{IP}\tau = ENC_{PS}^2 + ENC_{PD}^2 + ENC_{PP}^2. \quad (12)$$

It is worthwhile to observe that this equation, not explicit in (2), highlights three contributions to the parallel noise: ENC_{PS} from the system (dielectrics distributed among the detector, PCB/interconnections, and preamplifier), ENC_{PD} originated from the detector, and ENC_{PP} originated in the FEE and the detector together. Equation (12) highlights how the parallel noise cannot be reduced to the detector dark current alone, but all the parts of the system (detector, interconnection, FEE) contribute to it.

D. Series Noise Component: A System View

Starting from (2), the series noise component is generally written as (5) emphasizing the dependence of ENC_S on the signal processing time τ, indicating the $1/\tau$ dependence of the white series noise and the independence of the $1/f$ noise component of τ. In the following, it is shown how some interesting peculiarities of these noise components, not clearly and immediately visible in (5), can be well-underlined elaborating (5) in two other different forms.

Considering (3), (5) can rewritten as follows:

$$ENC_S^2 = A_S(C_D + C_C + C_P)^2 = ENC_{S1}^2 + ENC_{S2}^2 + ENC_{S3}^2 + ENC_{S4}^2 \quad (13)$$

with A_S given by

$$A_S = A_1 S_V \frac{1}{\tau} + A_2 2\pi A_f \quad (14)$$

and

$$\begin{aligned} ENC_{S1} &= \sqrt{A_S\left(C_D^2 + C_C^2 + C_P^2\right)} \\ ENC_{S2} &= \sqrt{2A_S C_D C_C} \\ ENC_{S3} &= \sqrt{2A_S C_D C_P} \\ ENC_{S4} &= \sqrt{2A_S C_C C_P}. \end{aligned} \quad (15)$$

Equation (13) highlights that ENC_S can be seen as the quadratic sum of four components involving all the elements of the detection system in a mixed form. For example, the value of the second component ENC_{S2} is determined by the

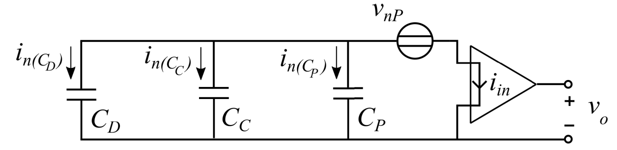

Fig. 2. Voltage fluctuation v_{nP} at the preamplifier input (hereby modeled with an ideal current input per effect of the adopted charge integrating configuration) generates three current noises $i_{n(C_D)}, i_{n(C_C)}, i_{n(C_P)}$ flowing through C_D, C_C, C_P, respectively.These three noise currents are fully correlated and become responsible of the four components of ENC_S as expressed by (13).

FEE for A_S, the detector for C_D and the interconnection for C_C, all together, and it is not possible to attribute this noise contribution to a single part of the system. It is worthwhile to note that in all cases where the C_D, C_C, and C_P values are close each other as, for example, in system using Semiconductor Drift Detectors or Pixel Detectors, the four values derived by (15) are very similar.

The physical meaning of the four components given by (15) is the following: the voltage fluctuations at the preamplifier input, due to the series noise source, act across the three parallel capacitances C_D, C_C, and C_P, generating three fully correlated noise currents which sum together producing the output noise (see Fig. 2). If these three currents were uncorrelated only the first noise term ENC_{S1} would exists, but because of the full correlation, the additional three terms $ENC_{S2}, ENC_{S3}, ENC_{S4}$ arise.[2]

Equations (13) and (15) show that the series component ENC_S is determined by all the three different parts of the detection system—detector, preamplifier, and interconnection—in such a manner that it is not possible anymore to separate them, and it is allowed to refer to it only as a system noise.

E. ENC_S: Detector and Interconnection Influence

In the particular case in which ENC_S is the dominant noise component in the system, as it can occur at low operating temperatures or at shaping times much shorter that the optimum one, the influence of the detector and interconnection capacitances can be more easily seen and quantified. In fact it is not necessary to consider ENC_S^2 for summing it to the parallel noise component; this allow to directly examine ENC_S, which can be rewritten from (5) and (3) as follows:

$$ENC_S = \sqrt{A_S}C_D + \sqrt{A_S}C_C + \sqrt{A_S}C_P \quad (16)$$

which emphasizes that ENC_S is determined by three addenda, whose weights, for each given shaping time, are determined by the detector, interconnection, and preamplifier capacitance, respectively. The common factor $\sqrt{A_S}$ [see (14)] depends only on parameters of the FEEs (preamplifier and shaper) but the detector and interconnection are also jointly responsible for ENC_S, in fact, the first and second terms null for an ideal detector ($C_D = 0$) or an ideal interconnection ($C_C = 0$), while are significant or even dominant in all real cases. It is worthwhile to underline that those capacitances, in conjunction with the preamplifier series voltage noise, becomes sources of

[2]The r.m.s. value of a current noise i sum of two components i_1, i_2 is $i_{\text{rms}}^2 = i_{1\text{rms}}^2 + i_{2\text{rms}}^2 + 2c(i_{1\text{rms}} i_{2\text{rms}})$ in which $c = \overline{i_1 i_2}/i_{1\text{rms}} i_{2\text{rms}}$ is the correlation coefficient. $c = 0$ or $|c| = 1$ in case of uncorrelated and fully correlated quantities, respectively [37].

current noises, so being directly and equally responsible of the degradation of the S/N of the system. Equations (13) and (16) underline and quantify this explicitly.

IV. *ENC* Dependence on Capacitances

A. Introduction

The analysis presented in Section-III has shown how the capacitive components of the detector, interconnection, and preamplifier can significantly determine the system noise. It was so a common practice to characterize a preamplifier measuring the ENC_{EN} with increasing values of the capacitance loading its input, simulating increasing detector capacitances. Under the particular condition in which the ENC_S is the main component of the system noise and the detector capacitance C_D is dominant with respect to $C_C + C_P$, the dependence of ENC_{EN} on C_D is linear [(2) and (16)], so that the *ENC* versus C graph can be fit to the equation

$$ENC_{\text{EN}}(C_D) = ENC_{\text{EN}}(0) + \left(\frac{dENC_{\text{EN}}}{dC_D}\right) C_D \tag{17}$$

in which $ENC_{\text{EN}}(0)$ is the ENC_{EN} measured with the preamplifier input floating, and $dENC_{\text{EN}}/dC_D$ is the so-called "noise slope" of the preamplifier.

B. General Equation for the Noise Slope

A general model for the noise slope $dENC_{\text{EN}}/dC_D$ can be derived considering not only the variation of the series noise component ENC_S with the input capacitance, but also the dependence of the parallel component ENC_P to the capacitances due to dielectric noise as expressed in (9). In addition, since the dielectric loss of each capacitance C_i (with $i = D, C, P$) can be different, it is useful to know how much ENC_{EN} can vary with respect to each C_i, which can be evaluated from (4) as follows:

$$\frac{\partial ENC_{\text{EN}}}{\partial C_i} = \left(\frac{1}{2ENC_{\text{EN}}}\right)\left(\frac{\partial ENC_S^2}{\partial C_i} + \frac{\partial ENC_P^2}{\partial C_i}\right) \tag{18}$$

from (13) and for any i

$$\frac{\partial ENC_S^2}{\partial C_i} = 2A_S C_T \tag{19}$$

which indicates that the slope of the series noise component is the same independently of which capacitance is actually varying. From (9) it results

$$\frac{\partial ENC_P^2}{\partial C_i} = A_2 2kTD_i \tag{20}$$

so that the slope of the parallel noise component can be very different depending on which capacitance is varying.

Considering (19) and (20), (18) results

$$\begin{aligned}\frac{\partial ENC_{\text{EN}}}{\partial C_i} &= \left(\frac{2A_s C_T + A_2 2kTD_i}{2ENC_{\text{EN}}}\right)\\ &= \left(\frac{ENC_S}{C_T}\right)\left(\frac{ENC_S}{ENC_{\text{EN}}}\right) + \left(\frac{ENC_{Di}}{2C_i}\right)\left(\frac{ENC_{Di}}{ENC_{\text{EN}}}\right)\\ &= \sqrt{A_S}\left(\frac{ENC_S}{ENC_{\text{EN}}}\right) + \sqrt{\frac{A_2 kTD_i}{C_i}}\left(\frac{ENC_{Di}}{ENC_{\text{EN}}}\right)\end{aligned} \tag{21}$$

in which ENC_{Di} is the dielectric noise contribution of C_i as given by (9). Some considerations on the slope $\partial ENC_{\text{EN}}/\partial C_i$ can be drawn from (21).

1) It is given by the weighted sum of the slope (ENC_S/C_T) due to the series noise component and the slope $(ENC_{Di}/2C_i)$ of the dielectric noise component.
2) It depends on the processing time τ since both ENC_{EN} as ENC_S depend on it. Specifically, the slope increases with the shortening of τ where ENC_S becomes significant.
3) It is parameter proper of the system, not specific to the preamplifier alone, as it depends on all the factors determining ENC_{EN}, which includes detector, interconnection, and pulse shaping, as well.
4) In case the series noise ENC_S is the dominant component and ENC_{Di} can be neglected, (21) gives

$$\begin{aligned}\frac{\partial ENC_{\text{EN}}}{\partial C_i} &\cong \left(\frac{ENC_S}{C_T}\right) = \sqrt{A_S}\\ &= \sqrt{A_1 S_V \frac{1}{\tau} + A_2 2\pi A_f}\end{aligned} \tag{22}$$

so that A_S, given by (14), determines the constant slope of ENC_{EN} with respect to the variation of any capacitance C_i. In particular, it can be observed that A_S increases with the increase of the power spectral densities of the series voltage white noise (S_V) and $1/f$ noise (A_f) of the preamplifier. In case of CMOS preamplifiers, S_V increases with the decreasing of the gate width W and the drain current I of the input transistor, which are design requirements for low capacitance detectors or for low power consumption preamplifiers [45]. The $1/f$ noise coefficient A_f increases with the decreasing of W and it is proportional to $\sqrt{I}$ or independent of I according with the Hooge ($\Delta\mu$) or Mc Worther (ΔN) $1/f$ noise models, generally valid for p-channel and n-channel MOSFETs in strong inversion, respectively [45]. So, it is expected that system designed for very low capacitance detectors, such as semiconductor pixel or drift detectors, will be characterized by a high value of the noise slope. However, the traditional unit of measure (electrons r.m.s.)/pF for the noise slope can be even unconvenient or misleading in case of such detectors, whose capacitance variations can be expected below few tens of fF.

C. Sensitivity of ENC to Capacitances

The noise slope $dENC_{\text{EN}}/dC_D$ in (17) was commonly used since the beginning of nuclear electronics because of the historical reason that the few available preamplifiers were supposed to be used with different detectors within a relatively wide range of capacitances, and the ENC_{EN} versus C_D data were essential to the users to predict the final *ENC* with their own detector [15], [22], [38]. From 1980's, the situation strongly changed with the increasing use of microelectronics technology for manufacturing the FEEs, which started to be more and more custom designed for each specific detector and application [39], [40]. Some noticeable examples of FEE noise optimization in CMOS technologies can be found in [41] and [42]. Thus, nowadays, it makes no sense to use the same preamplifier for detectors with very different capacitances, so that the noise slope $dENC_{\text{EN}}/dC_D$ assumes a different

significance and importance: it can be now used to predict the dispersion of *ENC* in multi-channel systems or within large volume productions in the case that a certain dispersion of the input load capacitance around its nominal value is expected. At this aim, more effective and useful parameters should be the system sensitivities S_{C_i} with respect to input load capacitances (detector, interconnection and preamplifier), defined as follows:

$$S_{C_i} = \frac{\partial ENC_{\mathrm{EN}} / ENC_{\mathrm{EN}}}{\partial C_i / C_i} \tag{23}$$

which directly gives the relative variation of the system electronic noise for a given relative variation of each C_i. From (21) the equations for S_{C_i} can be directly derived as follows:

$$S_{C_i} = \left(\frac{C_i}{C_T}\right)\left(\frac{ENC_S^2}{ENC_{\mathrm{EN}}^2}\right) + \frac{1}{2}\left(\frac{ENC_{Di}^2}{ENC_{\mathrm{EN}}^2}\right). \tag{24}$$

As an example: in case of dominat series noise, it becomes $S_{Ci} \cong C_i/C_T$, which gives $S_{C_D} = S_{C_P} = 0.5$ in the particular case of negligible interconnection capacitance and under capacitive matching condition $C_P = C_D$.

V. Intrinsic FEE Noise

A. Definition and Utility

Dealing with a system composed by three main parts (detector, connection, and FEEs), it would be useful to have a methodology to quantify the contribution of each part to the overall noise of the system. However, it has been already shown in Section III-D that the system's noise cannot be reduced to a simple combination of three noise contributions, but a "system effect" is involved. Nevertheless, it is shown in this section that it is possible to extract some information by measuring the noise isolating one part of the system, the preamplifier, from the other two.

In case the noise is measured with the preamplifier input floating, with no connection to the PCB and/or to the detector, the ENC_{EN} [see (2)] reaches the minimum value because $ENC_{PD} = 0$ in the parallel component [see (12)], ENC_{PS} is at its lowest value (minimum dielectric is present), and ENC_{PP} is minimum as well because it includes only the preamplifier noise; in addition, the series component ENC_S is minimized due to $C_D = C_C = 0$ [see (13)]. The measured ENC_{EN} under this condition can be named as the *intrinsic electronic noise* of the FEE, indicated with $ENC_{\mathrm{EN}(i\mathrm{FEE})}$, because it is a feature belonging to the FEE alone, with no influence from any other element. $ENC_{\mathrm{EN}(i\mathrm{FEE})}$ coincides with $ENC(0)$ in (17) if the preamplifier input is effectively floating and not connected to anything on the PCB.

The intrinsic FEE electronic noise is a useful measurable quantity for two reasons. The first is that it gives the ultimate limit of ENC_{EN} theoretically reachable if the readout electronics is connected to an ideal detector ($I_D = 0$ and $C_D = 0$) by means of an ideal interconnection ($C_C = 0$). Although this situation is only ideal and it can never be reached, the intrinsic FEE noise is anyhow significant because it can be practically used to experimentally quantify the effect of the detector and interconnection when they are coupled to the preamplifier, so giving a quantitative evaluation on how much the real system is far from an ideal one. Moreover, the comparison between the system noise and the FEE intrinsic noise can help to identify, disentangle, and quantify some noise contributions, as demonstrated in Sections V-B–V-D, and this is the second reason of its utility.

B. Relationship Between Intrinsic FEE and System Noise

The FEE intrinsic noise can be written according to (4)

$$ENC_{\mathrm{EN}(i\mathrm{FEE})} = \sqrt{ENC_{S(i\mathrm{FFE})}^2 + ENC_{P(i\mathrm{FEE})}^2} \tag{25}$$

in which the series white and parallel noise components can be easily extracted by the experimental data, while the series $1/f$ and the parallel dielectric noise are mixed in the τ-independent component.

When the FEE is connected to the detector, the system is realized and its ENC_{EN} is related to $ENC_{\mathrm{EN}(i\mathrm{FEE})}$ as follows:

$$ENC_{\mathrm{EN}} = \sqrt{(m+1)^2 ENC_{S(i\mathrm{FEE})}^2 + ENC_{P(i\mathrm{FEE})}^2 + ENC_{P(\mathrm{CON+DET})}^2} \tag{26}$$

in which $m = (C_D + C_C)/C_P$ is the matching factor and $ENC_{P(\mathrm{CON+DET})}$ is due to the parallel noise components related to the interconnection and the detector. So, a comparison between ENC_{EN} and $ENC_{i\mathrm{FEE}}$ can give useful information on the contributions of the interconnection and detector to the series and parallel noise (SPN) components of the system.

C. Example of Application

In the following example, it is considered a system composed by a small area silicon drift detector (SDD), a CMOS charge sensitive preamplifier (SIRIO), and a digital processor realizing a triangular pulse shaping. The system has been realized and tested achieving high performance in X-ray spectroscopy [43].

Fig. 3 shows the ENC_{EN} versus τ experimental data measured under two conditions: 1) the FEE input floating, so acquiring the intrinsic FEE noise $ENC_{\mathrm{EN}(i\mathrm{FEE})}$, which ranges from 5 down to 1.3 electrons r.m.s. and 2) after a direct connection with the detector through a short (<1 mm) 25 μm diameter wire bonding, so acquiring the system noise ENC_{EN} which ranges from a minimum 6 up to 10 electrons r.m.s. The increase of ENC_{EN} after the connection is due to noise components introduced by the detector current ($I_D \cong 1$ pA) and capacitance ($C_D \cong 30$ fF) and by the interconnection capacitance ($C_C \cong 15$ fF) [44] with their effect on the SPN components.

The preamplifier was designed to obtain minimum system ENC_{EN} achieved under capacitive matching condition $m = 1$ [45], [46], which is confirmed by the experimental data: in fact the system series noise ENC_S (white and $1/f$) is exactly double with respect to the intrinsic series noise $ENC_{S(i\mathrm{FEE})}$ as expected for $m = 1$. Once m and so the system series noise is obtained, by comparing the experimental data with (26), this last allows to obtain the parallel noise component of the system $ENC_{P(\mathrm{CON+DET})}$.

Fig. 3 and Table II show all the noise components extracted by analyzing the experimental data $ENC_{\mathrm{EN}(i\mathrm{FEE})}$ and ENC_{EN}

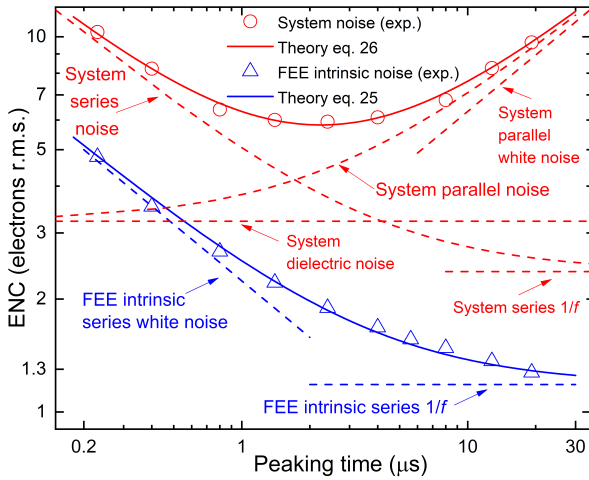

Fig. 3. Experimental *ENC* measured with the floating FEE input, so determining the intrinsic *ENC* and with the detector connected. The experimental data are fit to the theoretical equation and the different noise components are determined.

TABLE II
SYSTEM AND INTRINSIC NOISE COMPONENTS

Noise component	*ENC* (electrons r.m.s.)[a]	Percentage
Front-End Electronics		
Intrinsic series white	1.50	61.8
Intrinsic series $1/f$	1.18	38.2
Total intrinsic noise	1.91	100.0
System		
Series white	2.99	26.5
Parallel white	2.99	26.5
Series $1/f$	2.37	16.5
Parallel dielectric	3.22	30.5
Total system noise	5.83	100.0

[a]The white noise components are evaluated at the optimum peaking time of τ_{peak}=2.23 μs.

with (25) and (26) under the hypothesis that the parallel noise of the preamplifier due to dielectric loss is negligible, as then confirmed. The most interesting conclusion of this analysis is that the system noise is strongly affected by a significant contribution due to dielectric noise, which would otherwise be difficult to identify and quantify without the knowledge of the FEE intrinsic noise. The measured dielectric noise of 3.2 electrons r.m.s., arising after connecting the detector to the preamplifier, can be explained with a $D \cong 10^{-3}$ of the total added capacitance [26]. The lossy dielectric can be associated with the SiO_2 surrounding the detector's output electrode, but it cannot be excluded that even the semiconductor bulk, when depleted by mobile charges, can be a source of dielectric noise [47].

A direct analysis of the system ENC_{EN} by fitting to (2) would allow to extract the series and parallel white components but it cannot separate the τ-independent component in its $1/f$ and dielectric noise parts, as possible with the knowledge of the FEE intrinsic noise. Moreover, it can be appreciated how the FEE intrinsic noise allows to determine how close is the system to the capacitive matching condition, i.e., to its minimum noise, and which are the eventual dominant noise components on which the attention must be concentrated.

D. Final Considerations

It is worthwhile to highlight that the FEE is always designed to optimize the system performance considering all the elements and the noise components, that is the detector capacitance and leakage current and the estimated interconnection capacitance. Thus, the intrinsic noise of FEE must not considered as a figure of merit in itself, but it is useful if refereed to the system. Practically, the FEE intrinsic noise can be easily measured before assembling all the system and the best case for the system noise can be predicted to be with $ENC_{\mathrm{EN}} \cong 2ENC_{S(i\mathrm{FEE})}$ as derived from (26) under capacitive matching condition $m = 1$ and negligible parallel noises.

VI. Other Detector's Electronic Noise Contributions

In addition to the noise contributions to ENC_{EN} due to the detector, already considered in Section III, there are other noise components whose origin is in the detector itself and it is related to the generation and to the transport processes of the signal electric charge. The effect of these noise sources on the S/N of the system is discussed in Sections VI-A–VI-C subsections, showing also their close relationship and interaction with the electronic noise analyzed in the previous paragraphs. General remarks on these noise sources are presented in Section VI-C.

A. Electronic Noise Related to the Signal Charge Generation

The generation of charge from ionizing radiation is a complex process with a fundamental statistical nature and shows an intrinsic fluctuation present in all detectors made with any known semiconductor [48], [49]. Specifically, the signal charge generated by the absorption of an energy E from an ionizing particle or photon, is subjected to an intrinsic fluctuation which is commonly named *Fano noise* and gives an additional component to the system total noise, which can be expressed in terms *Noise Charge* NC_{GS} associated with the generation statistics (GS)

$$NC_{GS} = q\sqrt{F\left(E/\varepsilon\right)}\ [\mathrm{C}] \quad (27)$$

in which E is the energy transferred by the photon or particle to the semiconductor, ε [eV] is the electron-hole pair generation energy and F is the Fano factor, which quantifies the observed reduction ($F < 1$) of statistical fluctuations in the number of generated charge carriers with respect to pure Poisson statistics [10]. It is worthwhile to note that the term "Equivalent" is not appropriate in the case of Fano noise because it is a native charge fluctuation at the detector output/FEE input.

Since the electronic and Fano noises are uncorrelated, they can be quadratically summed to give a more complete *ENC* ENC_{ENF} including Fano

$$ENC_{\mathrm{ENF}}(E) = \sqrt{ENC_{\mathrm{EN}}^2 + NC_{GS}^2}\ [\mathrm{C}]. \quad (28)$$

Since NC_{GS} depends on the energy E, ENC_{ENF} is dependent on the signal amplitude itself, although also ENC_{EN} can depend on the signal in case of presence of non-stationary noise component as discussed in Section III-B. Equation (28) is quite important in the experimental characterization of a

system because it allows revealing anomalies related to additional noise components, as shown in the following. In fact, $ENC_{\mathrm{ENF}}(E)$ can be experimentally measured from the FWHM of the spectral lines at different photon/particle energy E; ENC_{EN} is obtained from the measured FWHM of the pulser line, and NC_{GS} calculated from (27). If the experimentally measured ENC_{ENF} does not obey (28), it means that the system is affected by additional noise or disturbance components such as: 1) charge trapping phenomena in the detector; 2) ballistic deficit; 3) fluctuation or drift in the pulser signal; 4) charge losses due to interaction of the photons in critical active volumes (edges of the detector, edge of the collecting electrode, close to surface or to geometrical interfaces); and 5) time-dependence of the conversion gain of the readout electronics. An example of this can be seen in Fig. 4 showing the experimental FWHMs of the Pulser and of the 5.9 keV ^{55}Fe spectral lines, as acquired with a non-collimated SDD coupled to a CMOS charge sensitive preamplifier and processed with a triangular shaper. The dashed line is the theoretical 5.9 keV line FWHM $= 2.35\varepsilon(ENC_{\mathrm{EFN}}/q)$ calculated summing the electronic and Fano noises as in (28). It can be noted that the measured FWHM of the 5.9 keV ^{55}Fe line is higher, indicating that additional phenomena, not related to the electronic or GS noises, are affecting the system, a problem that cannot be discovered if the electronic noise ENC_{EN} is not measured by means of the acquisition of a pulser line during the system characterization. For example, if the problem is related to a long charge induction time (see Section VI-B3), it could be sufficient to change the type of pulse shaping from triangular to trapezoidal, to reduce ballistic deficit effects.

B. Electronic Noise Related to the Signal Charge Transport

The transport of the signal charge through the detector active volume toward the collecting electrode can be a source of noise having three origins: trapping, detrapping, and induction phenomena, as discussed in Sections VI-B1–VI-B4. These noise components can be more or less relevant depending on the semiconductor used, the detector size, the experimental conditions, and the signal and noise levels. But, in general, their effect cannot be neglected a priori even in detector made of high purity semiconductors.

1) Charge Trapping Electronic Noise: During the transport, loss of charge carriers can occur due to the trapping centers for electrons and holes in the semiconductor. This loss of charge is commonly quantified by a measurable quantity called charge collection efficiency (CCE) defined as the ratio between the mean signal charge induced at the detector output electrode and the mean charge generated by the photon/particle CCE $= Q_{\mathrm{ind}}/Q_{\mathrm{gen}}$ [50]. The charge trapping has two effects on the performance of the system. The first effect is the reduction of signal amplitude, which causes a decrease of the signal-to-noise ratio implying loss of energy/position/timing resolution. This effect is generally seen and evaluated as equivalent to an increase in noise, as it is discussed in Section VII. The second effect is a widening and distortion of the spectral lines, due to the statistical nature of the trapping phenomenon, which involves a random quantity of captured carriers, different from event to event and, in case of photons, also strongly dependent where the photon has been absorbed. Sometimes, for simplicity, this trapping noise is considered as a Gaussian

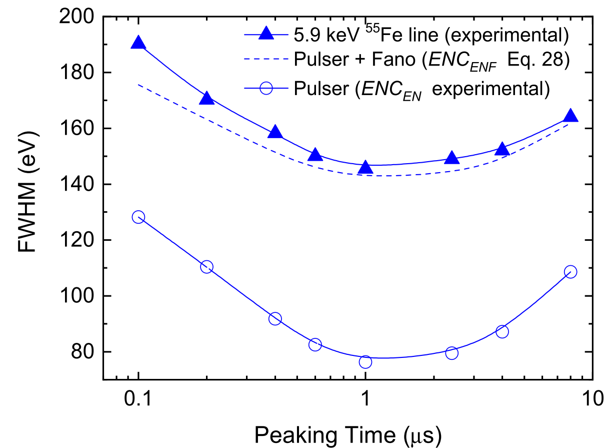

Fig. 4. Measured FWHM of the Pulser and 5.9 keV ^{55}Fe lines acquired with a SDD and a dedicated FEEs.

process and its associated Noise Charge NC_{TR} is quadratically summed to the electronic and generation noises [51], [52]. This procedure is a rough approximation because charge trapping generates a significant distortion of the spectral lines from a Gaussian shape, which become asymmetrical, as it is intuitive because the trapping is always a subtractive process on the original charge signal [50]. It has been demonstrated that the additional spectral line widening due to charge trapping depends not only on CCE but also on the electronic and Fano noises, so that higher ENC_{ENF} causes a higher excess line widening for the same CCE [53].

Effects of charge trapping have been observed both in detectors made with compound semiconductors as with germanium and silicon, due to several different causes as: significant defect or impurity density both native as due to radiation damage, presence of volumes with low electric field [54], [55], [56], [57], [58], [59], [60].

2) Charge Detrapping Electronic Noise: The trapped charges can escape from the trap with a given probability described by a characteristic detrapping time t_D. In case the trap density is high and t_D extremely long, the number of filled traps increases with time and a space charge can appear. This phenomenon, known as polarization, strongly affects the performance of the detector when it distorts the internal electric field increasing the charge collection time, lowering the CCE and the detector active volume [61]. In case of relatively short t_D, the trapping of signal charges is balanced by the detrapping process, and a stationary condition is reached. It is worthwhile noting that the detrapping phenomena is a source of noise as well, but its effect is different from the trapping noise. In fact, the electrons and holes generated by a given photon are partially trapped during their drift toward the collecting electrodes, so that the trapping events can be considered simultaneous, within the collection time interval, for all the trapped charges belonging to the same signal packet. Instead, the emission of a charge from a trap center occurs at times randomly distributed over a longer time scale, generating an excess detector mean dc current that can be calculated as follows:

$$I_{DT} = q\frac{\sum_i E_i R_i}{\varepsilon}(1 - \mathrm{CCE}) = q\frac{\overline{P}_{\mathrm{in}}}{\varepsilon}(1 - \mathrm{CCE}) \tag{29}$$

in which R_i (s^{-1}) is the absorption rate of photons/particles with energy E_i, and $\overline{P}_{\text{in}}$ (eV/s) represents the mean input energy rate and I_{DT} is $(1 - \text{CCE})$ times the total radiation generated current. Fig. 5 shows examples of the calculated values of I_{DT} as a function of the absorbed energy rate for CdTe and Si detectors with different values of CCE. It can be observed that significant values of detrapping currents can be reached when relatively high radiation rate are considered: for example, 100 keV photons at 10^6 counts per seconds (cps), give $\overline{P}_{\text{in}} = 10^5$ MeV/s, generating $I_{DT} = 0.3$ nA at CCE $= 0.9$ in CdTe. Even for Silicon detectors with very high CCE, I_{DT} could be significant at high energy rates if compared with typical dark currents of small area, cooled devices: 10 keV at 1 Mcps gives 10^4 MeV/s and $I_{DT} = 0.4$ pA at CCE $= 0.999$.

The detrapping process is a source of parallel noise which is expected to show a sum of Lorentzian spectral power densities, with characteristic frequencies determined by the detrapping times of the active trap centers. If many traps with different detrapping times are involved, a $1/f$ spectrum can be generated [62]. It is not immediate to measure this noise component because it is not associated with a "dark current" but it occurs when signal charge pulses are present at the detector output. Sampling and digital processing of the preamplifier output voltage could be used to observe a variation of the spectral density associated with the background level under dark and under exposed conditions. In any case, the effect of this additional noise can be seen in the acquired spectra as a worsening of energy resolution when the input energy rate increases.

3) Charge Induction Electronic Noise: The transport of signal charge through the detector generates, by charge induction, a current signal at the detector output electrode. The shape and duration in time of the induced current signal can be described, for a given trajectory of the charge carriers and weighting field of the output electrode, applying the Shockley–Ramo theorem [9], [63]. When the induction time (i.e., the time duration of the current pulse) is comparable to the shaping time, only part of the induced signal is integrated through the readout processing electronics, resulting in the *ballistic deficit* [9], [10], [64]. The main effect is the reduction of the amplitude of the shaper output signal, with a first consequence of lowering the S/N. In addition, under particular conditions, this signal reduction is subjected to fluctuations equivalent to a noise. This occurs when the induction time depends on the charge generation point and this is a statistical variable, as in case of absorption of photons in a diode, so a random fluctuation of the signal is expected as well.

This noise component can be significant in system using compound semiconductor detectors such as CdTe and CdZnTe because of the low mobility of holes [66], but also using very thick high purity germanium because of the relatively long charge collection time.

The same effect can be also significant in semiconductor drift detectors, in which the randomicity of the point of interaction of the photon/particle translates in a randomicity of the drift time and so on the duration of the signal current pulse at the anode, due to charge diffusion and electrostatic repulsion effects [65]. The final result is a widening and distortion of the spectral line, which can be experimentally quantified as for the trapping noise using (30), as shown in Section VI-B4.

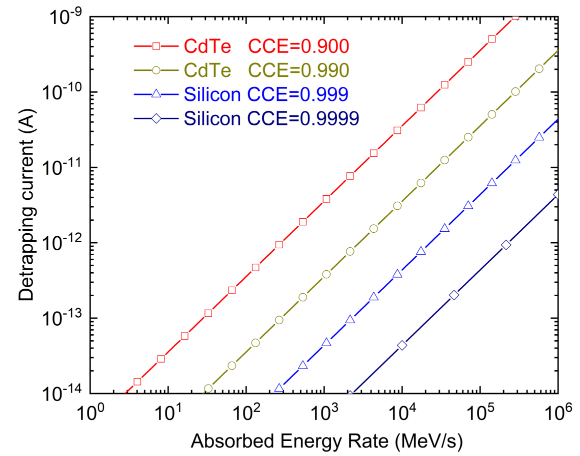

Fig. 5. Detrapping current versus Absorbed Energy Rate as given by (29) for CdTe and Silicon detectors with different values of the CCE.

4) Charge Transport Electronic Noise (Experimental): The noise related to the signal charge transport (trapping and/or induction) can be experimentally quantified in terms of excess linewidth as follows:

$$\text{FWHM}_{CT} = \sqrt{\text{FWHM}_{\text{EXP}}^2 - \text{FWHM}_{\text{ENF}}^2}\ [\text{eV}] \qquad (30)$$

in which FWHM_{EXP} is the measured FWHM of a particular spectral line and $\text{FWHM}_{\text{ENF}} = 2.35\varepsilon ENC_{\text{ENF}}/q$ with ENC_{ENF} given by (28). It is important to highlight that the trapping/induction noise, quantified by (30) is a complex function of ENC_{ENF} because the FWHM_{EXP} strongly depends on ENC_{ENF} itself as demonstrated in [53].

The effect of noise related to the signal charge transport, both trapping-detrapping and induction, can be easily observed in detectors based on some compound semiconductors, as CdTe and CdZnTe, in which the density of defects is high, and the hole mobility is relatively low [66]. Fig. 6 shows the 59.54 keV spectral line from ^{241}Am acquired with a CdTe detector coupled to a custom low-noise preamplifier [44]. The acquired pulser line has been artificially shifted below the 59.54 keV line for a direct comparison. The expected 59.54 keV line, if acquired with a detector without signal charge losses (due to trapping and ballistic deficit), is calculated from (28) and drawn as a dashed line. The widening and distortion of the 59.54 keV line can be very clearly seen. Considering that the electronic noise gives $\text{FWHM}_{\text{EN}} = 360$ eV, the GS noise $\text{FWHM}_{GS} = 419$ eV, a noise related to the charge transport equivalent to $\text{FWHM}_{CT} = 586$ eV can be calculated by means of (30), which is the dominant noise contribution.

C. Generation and Transport Electronic Noises: Final Remarks

In addition to noise associated with the dark current and the contributions due to its capacitance, four other detector-related noise sources have been considered: one related to the generation (Fano) and three related to the transport of signal charges (trapping, detrapping, and induction). It is useful to point out some final observations about these noise sources. In the first

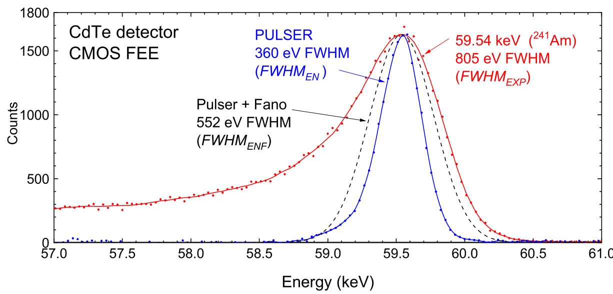

Fig. 6. 59.54 keV spectral line from ^{241}Am acquired with a CdTe detector coupled to a CMOS preamplifier. The acquired Pulser line has been artificially shifted below the 59.54 keV line for comparison. The expected 59.54 keV line if acquired with a detector without signal charge losses is calculated and drawn in dashed line. The effect of widening and distortion of the 59.54 keV line can be very clearly seen.

place, both the charge generation and the transport processes introduce random fluctuations of the electric signal amplitude, widening the spectral lines. In this respect, they can be indeed considered electronic noise sources. Anyhow, there is a fundamental difference between the generation and transport-related noises (GTNs) and the SPNs considered in Section III. SPNs have an external and independent origin with respect to the signals and superpose to the signals themselves, while GTN have their origin in the signal formation process itself, so they cannot be filtered as done for SPNs. In other words, the detector charge signal is generated through processes which are intrinsically noisy due to their statistical nature, so that these noises (i.e., random fluctuations) are not added to a pure signal but, in a certain sense, they are natively incorporated into the signal itself, and the pure signal does not exist since the beginning so that it cannot be recovered by filtering. For example, the generation noise cannot be filtered or attenuated at all and sets the ultimate limit of the S/N of a detection system, commonly called "Fano limit." For this reason, it is useful and practical to consider the GTN separately from the electronic noise quantifying ENC_{EN} with (2), then accounting the generation noise with (28) and the trapping, detrapping and collection noise with (30).

The noise associated with the charge transport (trapping and induction) has also some peculiarities. The *trapping noise* depends on the type and volume density of the trapping centers and so it is strictly related to the purity and defect density of the crystal. In addition, the trapping noise depends also on the electrons and holes transit times ($t_{tr,n}$, $t_{tr,p}$) required to reach the electrodes because the longer t_{tr}, the higher the probability that a charge carrier will be trapped.

The noise associated with the signal induction process also depends on t_{tr} since it determines the induction time. A fluctuation due to the ballistic deficit arises when the signal induction time is comparable to the signal shaping time, so these fluctuation can be effectively reduced by setting longer shaping times or increasing the flat-top in trapezoidal shaping. Trapping and induction noises are strictly related to the size of the detector in the direction of the drift field (bulk thickness in case of diode-line devices, bulk length in case of drift detectors) and on the detector internal drift field. The requirement of thick semiconductors for realizing efficient detectors for high energy radiation can lead to increased trapping noise. The same occurs for high-Z compound semiconductors (GaAs, CdTe, CdZnTe, TlBr, ...) whose high efficiency in X and γ-ray absorption is paid in terms of a lower crystal purity and higher lattice defect density. In addition, most compound semiconductors show a relatively low mobility of holes, which increases both the trapping and induction noises. Finally, the possibility to operate the detector at high internal electric field in order to maximize the carrier velocity, so minimizing $t_{tr,n}$ and $t_{tr,p}$, is in conflict with the increase of the detector dark current with the increasing of the bias voltage.

VII. Concept of Equivalent Noise Energy

The electronic noise of a detection system is generally indicated using the *ENC* (Coulomb), defined as described in Section II, but commonly expressed also in different units of measure, specifically electrons r.m.s. or eV FWHM, by simply multiplying *ENC* by a proper converting constant. In some publications, the term equivalent noise energy (ENE) has been used simply to indicate the *ENC* when expressed in eV [67], [68]. Actually, a concept of ENE can be more properly defined with a stronger link to all elements involved in the specific detection system under analysis, and not simply as synonymous of *ENC*.

The classical definition of *ENC* given in Section II considers only the electronic noise as evaluated by (2), excluding the generation and transport noise contributions, although these can be significant, or even dominant, in determining the energy resolution of a detection system. This limitation is intrinsic to the *ENC* definition since the r.m.s. voltage noise at the shaper output is independent by the fluctuations of the signal amplitude and shape generated internally to the detector. As far as the GS noise is concerned, this limit is overcome by quadratically adding the Fano noise to the electronic noise contribution as stated with (28), thanks to the Gaussian nature of the generation noise. In addition, the concept of *ENC* assumes the detector-output/preamplifier-input electrode as system's input and the charge injected into this electrode as input signal. Actually, the input signal of a radiation detection system can be more realistically assumed as the energy E deposited by the photon/particle into the detector itself, so that, for analogy, it is possible to define an ENE to quantify the noise of a system as referred to its real input. Considering the relationship between the photon/particle energy E and the mean value of the charge signal Q_{ind} induced at the detector output

$$Q_{\mathrm{ind}} = q\left(\frac{E}{\varepsilon}\right)\mathrm{CCE} \tag{31}$$

the ENE, expressed in eV r.m.s., is the energy E that generates a signal at the output of the shaper whose mean amplitude is equal to the r.m.s. value of the noise at the shaper output itself, and so produces a mean induced charge $Q_{\mathrm{ind}} = ENC_{\mathrm{EN}}$, which substituted into (31) gives

$$\mathrm{ENE} = \frac{\varepsilon ENC_{\mathrm{EN}}}{q\mathrm{CCE}}\ (\mathrm{eV}). \tag{32}$$

The ENE concept, as defined and expressed by (32), includes also an exclusive property of the detector, the CCE, so having the advantage, over the *ENC* (also when expressed in eV), to highlight the role of the detector and the electronics in the detection system at the same time. In addition, ENE given by (32) is useful to compare detectors made with different semiconductors and different CCE. For example, the same electronic noise ENC_{EN} generates relatively larger spectral lines, explicated with larger ENE, in case of detectors with higher ε or lower CCE, as (32) predicts. It has to be pointed out that the ENE as defined with (32) does consider the effect of the mean charge loss due to trapping phenomena, through CCE, but does not include the effect of ballistic deficit. Moreover, it has to be considered that the CCE $= Q_{\mathrm{ind}}/Q_{\mathrm{gen}}$, ratio between the induced and the generated charge, is a function of the coordinates (x, y, z) where the charge is generated in the detector so it depends on the photon energy or on the type and energy of the particle. The CCE in (32) is the experimentally measured value which is a weighted mean value of CCE (x, y, z) for a given photon/particle [50]. It has to be considered that the FWHM of the pulser, calibrated in eV using a spectrum of a known radiation source acquired by a given detector, corresponds always to the ENE defined as in (32) while only in case of CCE $= 1$ is equal to the *ENC* expressed in eV. This has to be considered for all semiconductor detectors for which the CCE is not known because not measured.

VIII. Conclusion

The problem of the electronic noise in radiation detection systems based on semiconductor detectors has been analyzed with a unified approach, highlighting the roles of the detector, the interconnection, and the FEEs, and their interactions in determining the overall performance. It has been shown how, once the detector is connected to the FEE, the electronic noise cannot always be separated in independent components associated with each specific part, but a system level view is necessary. In particular, dielectric noise and series voltage noise must be always considered as *system noise* components. It has been shown how the intrinsic noise of the electronics, measurable when the preamplifier input is left floating, can be useful to determine the ultimate noise limit and the contribution of the additional noise components when the detector is connected to the FEE, in particular the dielectric noise. The electronic noise contributions from the detector arising from the charge transport phenomena as charge trapping, detrapping, and induction, have been analyzed, in addition to the noise contributions from the dark current and charge generation. It has been discussed how to take into account the trapping and the induction noise, which does not quadratically sum to the others, as sometimes erroneously done. This unified approach not only better clarifies the theoretical problem but also offers the advantage of analyzing the experimental data more precisely, permitting the identification of weak spots of the system noise to better optimize its performance. Although developed considering semiconductor detectors, the analysis and the method can be easily extended also to other types of detectors.

Acknowledgment

The authors thanks A. Pullia for reading the manuscript and for his advice and the reviewers and the editor for their detailed comments and fruitful discussion.

References

[1] W. C. Elmore and M. Sands, *Electronics—Experimental Techniques*. New York, NY, USA: McGraw-Hill, 1949.
[2] A. B. Gillespie, *Signal, Noise and Resolution in Nuclear Counter Amplifiers*. London, U.K.: Pergamon, 1953.
[3] E. Baldinger and W. Franzen, *Advances in Electronics and Electron Physics*, vol. 8. New York, NY, USA: Academic, 1956, p. 255.
[4] R. C. Jones, "Noise in radiation detectors," *Proc. IRE*, vol. 47, no. 9, pp. 1481–1486, 1959.
[5] F. T. Arecchi, G. Cavalleri, E. Gatti, and V. Svelto, "Signal to noise ratio and resolving time in pulse amplifiers for nuclear detectors," *Energia Nucleare*, vol. 7, no. 10, pp. 691–696, Oct. 1960.
[6] E. Gatti and V. Svelto, "Resolution as a function of noise spectrum in amplifiers for particles detection," *Energia Nucleare*, vol. 8, no. 8, pp. 505–509, Aug. 1961.
[7] G. Bertolini and A. Coche, *Semiconductor Detectors*. Amsterdam, The Netherlands: North Holland, 1968, ch. 3.
[8] P. W. Nicholson, *Nuclear Electronics*. London, U.K.: Wiley, 1974.
[9] E. Gatti and P. F. Manfredi, "Processing the signals from solid-state detectors in elementary-particle physics," *La Rivista del Nuovo Cimento*, vol. 9, no. 3, pp. 1–146, 1986.
[10] G. F. Knoll, *Radiation Detection and Measurement*, 4th ed. Hoboken, NJ, USA: Wiley, 2010.
[11] V. Radeka, "Low-noise techniques in detectors," *Annu. Rev. Nucl. Part. Sci.*, vol. 38, no. 1, pp. 217–277, Dec. 1988.
[12] E. Gatti, M. Sampietro, and P. F. Manfredi, "Optimum filters for detector charge measurements in presence of noise," *Nucl. Instrum. Methods Phys. Res. A, Accel. Spectrom. Detect. Assoc. Equip.*, vol. 287, no. 3, pp. 513–520, Feb. 1990.
[13] E. Gatti, P. F. Manfredi, M. Sampietro, and V. Speziali, "Suboptimal filtering of $1/f$-noise in detector charge measurements," *Nucl. Instrum. Methods Phys. Res. A, Accel. Spectrom. Detect. Assoc. Equip.*, vol. 297, no. 3, pp. 467–478, Dec. 1990.
[14] B. B. Rossi and H. H. Staub, *Ionization Chambers and Counters—Experimental Techniques*. New York, NY, USA: McGraw-Hill, 1949.
[15] C. Cottini, E. Gatti, G. Giannelli, and G. Rozzi, "Minimum noise preamplifier for fast ionization chambers," *Il Nuovo Cimento*, vol. 3, no. 2, pp. 473–483, Feb. 1956.
[16] K. G. McKay, "A. Germanium counter," *Phys. Rev.*, vol. 76, no. 10, p. 1537, Nov. 1949.
[17] S. S. Friedland, J. W. Mayer, and J. S. Wiggins, "The solid—State ionization chamber," *IRE Trans. Nucl. Sci.*, vol. 7, nos. 2–3, pp. 181–185, Jun. 1960.
[18] G. L. Miller, W. L. Brown, P. F. Donovan, and I. M. Mackintosh, "Silicon p-n junction radiation detectors," *IRE Trans. Nucl. Sci.*, vol. 7, nos. 2–3, pp. 185–189, Jun. 1960.
[19] R. T. Graveson and H. Sadowski, "Pulse amplifiers using transistor circuits," *IRE Trans. Nucl. Sci.*, vol. 5, no. 3, pp. 179–182, 1958.
[20] R. L. Chase, W. A. Higinbotham, and G. L. Miller, "Amplifiers for use with p-n junction radiation detectors," *IRE Trans. Nucl. Sci.*, vol. 8, no. 1, pp. 147–150, Jan. 1961.
[21] E. Fairstein, "Considerations in the design of pulse amplifiers for use with solid state radiation detectors," *IRE Trans. Nucl. Sci.*, vol. 8, no. 1, pp. 129–139, Jan. 1961.
[22] J. L. Blankenship, "Design of low-noise vacuum-tube pulse amplifiers for semiconductor radiation-detector spectroscopy," *IEEE Trans. Nucl. Sci.*, vol. NS-11, no. 3, pp. 373–381, Jun. 1964.
[23] W. Schottky, "Über spontane Stromschwankungen in verschiedenen Elektrizitätsleitern," *Annalen der Physik*, vol. 362, no. 23, pp. 541–567, 1918.
[24] J. B. Johnson, "Thermal agitation of electricity in conductors," *Phys. Rev.*, vol. 32, no. 1, pp. 97–109, Jul. 1928.
[25] G. Giacomini, "Fabrication of silicon sensors based on low-gain avalanche diodes," *Frontiers Phys.*, vol. 9, Apr. 2021, Art. no. 618621, doi: 10.3389/fphy.2021.618621.

[26] G. Bertuccio, A. Pullia, and G. De Geronimo, "Criteria of choice of the front-end transistor for low-noise preamplification of detector signals at sub-microsecond shaping times for X- and γ-ray spectroscopy," *Nucl. Instrum. Methods Phys. Res. A, Accel. Spectrom. Detect. Assoc. Equip.*, vol. 380, nos. 1–2, pp. 301–307, Oct. 1996.

[27] G. Bertuccio and A. Pullia, "A method for the determination of the noise parameters in preamplifying systems for semiconductor radiation detectors," *Rev. Sci. Instrum.*, vol. 64, no. 11, pp. 3294–3298, Nov. 1993.

[28] V. Radeka, "State of the art of low noise amplifiers for semiconductor radiation detectors," in *Proc. Int. Symp. Nuclear Electron.*, Versailles, France, Sep. 1968.

[29] V. Radeka, "Field effect transistors for charge amplifiers," *IEEE Trans. Nucl. Sci.*, vol. NS-20, no. 1, pp. 182–187, Feb. 1973.

[30] R. J. McIntyre, "Multiplication noise in uniform avalanche diodes," *IEEE Trans. Electron Devices*, vol. ED-13, no. 1, pp. 164–168, Jan. 1966.

[31] G. Bertuccio, L. Fasoli, and M. Sampietro, "Design criteria of low-power low-noise charge amplifiers in VLSI bipolar technology," *IEEE Trans. Nucl. Sci.*, vol. 44, no. 5, pp. 1708–1718, Oct. 1997.

[32] M. Manghisoni, "Gate current noise in ultrathin oxide MOSFETs and its impact on the performance of analog front-end circuits," *IEEE Trans. Nucl. Sci.*, vol. 55, no. 4, pp. 2399–2407, Aug. 2008.

[33] G. De Geronimo and P. O'Connor, "A CMOS detector leakage current self-adaptable continuous reset system: Theoretical analysis," *Nucl. Instrum. Methods Phys. Res. A, Accel. Spectrom. Detect. Assoc. Equip.*, vol. 421, nos. 1–2, pp. 322–333, Jan. 1999.

[34] M. Sampietro, G. Bertuccio, and L. Fasoli, "Current mirror reset for low-power BiCMOS charge amplifier," *Nucl. Instrum. Methods Phys. Res. A, Accel. Spectrom. Detect. Assoc. Equip.*, vol. 439, nos. 2–3, pp. 373–377, Jan. 2000.

[35] V. Radeka, "Signal processing for particle detectors," in *Particle Physics Reference Library: Volume 2: Detectors for Particles and Radiation*. Cham, Switzerland: Springer, 2011, pp. 466–470.

[36] F. Mele, J. Quercia, and G. Bertuccio, "Analytical model of the discharge transient in pulsed-reset charge-sensitive amplifiers," *IEEE Trans. Nucl. Sci.*, vol. 68, no. 7, pp. 1511–1518, Jul. 2021.

[37] A. van der Ziel, *Noise*. London, U.K.: Chapman & Hall 1955, p. 4.

[38] K. F. Smith and J. E. Cline, "A low-noise charge sensitive preamplifier for semiconductor detectors using paralleled field-effect-transistors," *IEEE Trans. Nucl. Sci.*, vol. NS-13, no. 3, pp. 468–476, Jun. 1966.

[39] R. Hofmann, G. Lutz, B. J. Hosticka, M. Wrede, G. Zimmer, and J. Kemmer, "Development of readout electronics for monolithic integration with diode strip detectors," *Nucl. Instrum. Methods Phys. Res. A, Accel. Spectrom. Detect. Assoc. Equip.*, vol. 226, no. 1, pp. 196–199, Sep. 1984.

[40] W. Buttler, B. J. Hosticka, G. Lutz, and P. F. Manfredi, "A JFET-CMOS radiation-tolerant charge-sensitive preamplifier," *IEEE J. Solid-State Circuits*, vol. 25, no. 4, pp. 1022–1024, Aug. 1990.

[41] P. Grybos, "Front-end electronics for multichannel semiconductor detector systems," Warsaw Univ. Technol. Publishing House, Warsaw, Poland, Tech. Rep. EuCARD-BOO-2010-004, 2010, vol. 8.

[42] P. O'Connor and G. De Geronimo, "Prospects for charge sensitive amplifiers in scaled CMOS," *Nucl. Instrum. Methods Phys. Res. A, Accel. Spectrom. Detect. Assoc. Equip.*, vol. 480, nos. 2–3, pp. 713–725, Mar. 2002.

[43] M. Sammartini et al., "Pixel Drift Detector (PixDD)—SIRIO: An X-ray spectroscopic system with high energy resolution at room temperature," *Nucl. Instrum. Methods Phys. Res. A, Accel. Spectrom. Detect. Assoc. Equip.*, vol. 953, Feb. 2020, Art. no. 163114.

[44] F. Mele, M. Gandola, and G. Bertuccio, "SIRIO: A high-speed CMOS charge-sensitive amplifier for high-energy-resolution X-γ ray spectroscopy with semiconductor detectors," *IEEE Trans. Nucl. Sci.*, vol. 68, no. 3, pp. 379–383, Mar. 2021.

[45] G. Bertuccio and S. Caccia, "Noise minimization of MOSFET input charge amplifiers based on $\Delta\mu$ and ΔN $1/f$ models," *IEEE Trans. Nucl. Sci.*, vol. 56, no. 3, pp. 1511–1520, Jun. 2009.

[46] A. Rivetti, *CMOS: Front-End Electronics for Radiation Sensors*. Boca Raton, FL, USA: CRC Press, 2015.

[47] M. Akiba, "$1/f$ dielectric polarization noise in silicon p-n junctions," *Appl. Phys. Lett.*, vol. 71, no. 22, pp. 3236–3238, Dec. 1997, doi: 10.1063/1.120301.

[48] C. A. Klein, "Bandgap dependence and related features of radiation ionization energies in semiconductors," *J. Appl. Phys.*, vol. 39, no. 4, pp. 2029–2038, Mar. 1968.

[49] R. Devanathan, L. R. Corrales, F. Gao, and W. J. Weber, "Signal variance in gamma-ray detectors—A review," *Nucl. Instrum. Methods Phys. Res. A, Accel. Spectrom. Detect. Assoc. Equip.*, vol. 565, no. 2, pp. 637–649, Sep. 2006.

[50] G. Bertuccio, A. Pullia, F. Nava, and C. Lanzieri, "Schottky junctions on semi-insulating LEC gallium arsenide for X- and γ-ray spectrometers operated at and below room temperature," *IEEE Trans. Nucl. Sci.*, vol. 44, no. 2, pp. 117–124, Apr. 1997.

[51] G. F. Knoll and D. S. Mcgregor, "Fundamentals of semiconductor detectors for ionizing radiation," in *Proc. Mat. Res. Soc. Symp.*, vol. 302, 1993, p. 302.

[52] A. Owens and A. Peacock, "Compound semiconductor radiation detectors," *Nucl. Instrum. Methods Phys. Res. A, Accel. Spectrom. Detect. Assoc. Equip.*, vol. 531, no. 1–2, pp. 18–37, Sep. 2004.

[53] G. Bertuccio, C. Canali, and F. Nava, "Energy resolution in GaAs X- and γ-ray detectors," *Nucl. Instrum. Methods Phys. Res. A, Accel. Spectrom. Detect. Assoc. Equip.*, vol. 410, no. 1, pp. 29–35, Jun. 1998.

[54] W. H. Dai et al., "Modeling the charge collection efficiency in the Li-diffused inactive layer of P-type high purity germanium detector," *Appl. Radiat. Isot.*, vol. 193, Mar. 2023, Art. no. 110638.

[55] J. Hayward and D. Wehe, "Incomplete charge collection in an HPGe double-sided strip detector," *Nucl. Instrum. Methods Phys. Res. A, Accel. Spectrom. Detect. Assoc. Equip.*, vol. 586, no. 2, pp. 215–223, Feb. 2008.

[56] M. Descovich et al., "Effects of neutron damage on the performance of large volume segmented germanium detectors," *Nucl. Instrum. Methods Phys. Res. A, Accel. Spectrom. Detect. Assoc. Equip.*, vol. 545, nos. 1–2, pp. 199–209, Jun. 2005.

[57] M. Gugiatti et al., "Characterisation of a silicon drift detector for high-resolution electron spectroscopy," *Nucl. Instrum. Methods Phys. Res. A, Accel. Spectrom. Detect. Assoc. Equip.*, vol. 979, Nov. 2020, Art. no. 164474.

[58] O. Tousignant et al., "Transport properties and performance of CdZnTe strip detectors," *IEEE Trans. Nucl. Sci.*, vol. 45, no. 3, pp. 413–416, Jun. 1998.

[59] N. Auricchio, L. Marchini, E. Caroli, A. Zappettini, L. Abbene, and V. Honkimaki, "Charge transport properties in CdZnTe detectors grown by the vertical Bridgman technique," *J. Appl. Phys.*, vol. 110, no. 12, Dec. 2011, Art. no. 124502, doi: 10.1063/1.3667201.

[60] L. Abbene et al., "Room-temperature X-ray response of cadmium-zinc-telluride pixel detectors grown by the vertical Bridgman technique," *J. Synchrotron Rad.*, vol. 27, pp. 319–328, Jan. 2020, doi: 10.1107/S1600577519015996.

[61] D. S. Bale and C. Szeles, "Nature of polarization in wide-bandgap semiconductor detectors under high-flux irradiation: Application to semi-insulating Cd_{1-x} Zn_xTe," *Phys. Rev. B, Condens. Matter*, vol. 77, no. 3, 2008, Art. no. 035205.

[62] A. L. McWorther, "$1/f$ noise and germanium surface properties," in *Proc. Conf. Phys. Semiconductor Surf.* Philadelphia, PA, USA: Univ. of Pennsylvania Press, Jun. 1956, pp. 207–228.

[63] S. Ramo, "Currents induced by electron motion," *Proc. IRE*, vol. 27, no. 9, pp. 584–585, Sep. 1939.

[64] B. W. Loo, F. S. Goulding, and D. Gao, "Ballistic deficits in pulse aping amplifiers," *IEEE Trans. Nucl. Sci.*, vol. 35, no. 1, pp. 114–118, Feb. 1988.

[65] E. Gatti, A. Longoni, P. Rehak, and M. Sampietro, "Dynamics of electrons in drift detectors," *Nucl. Instrum. Methods Phys. Res. A, Accel. Spectrom. Detect. Assoc. Equip.*, vol. 253, no. 3, pp. 393–399, Jan. 1987.

[66] M. Sammartini et al., "X-γ-ray spectroscopy with a CdTe pixel detector and SIRIO preamplifier at deep submicrosecond signal-processing time," *IEEE Trans. Nucl. Sci.*, vol. 68, no. 1, pp. 70–75, Jan. 2021.

[67] C. Cerri et al., "A current sensitive liquid argon calorimeter," *Nucl. Instrum. Methods Phys. Res. A, Accel. Spectrom. Detect. Assoc. Equip.*, vol. 227, no. 2, pp. 227–236, Nov. 1984.

[68] G. Bertuccio, "Prospect for energy resolving X-ray imaging with compound semiconductor pixel detectors," *Nucl. Instrum. Methods Phys. Res. A, Accel. Spectrom. Detect. Assoc. Equip.*, vol. 546, nos. 1–2, pp. 232–241, Jul. 2005.

Open Access funding provided by 'Politecnico di Milano' within the CRUI CARE Agreement